Geophysical Research Letters

RESEARCH LETTER
10.1029/2018GL080274

Key Points:
- We report the main characteristics of 30 three-belt events that occurred between 2012 and 2017 using Van Allen Probes data
- The formation of three-belt events is influenced by the magnetopause position, and their location correlates with *SYM-H* minimum index
- Three-belt events are observed from 1.8 to 7.6 MeV, and on average their decay rates get longer as energy increases

Supporting Information:
- Supporting Information S1

Correspondence to:
V. A. Pinto,
victor.pinto@gmail.com

Citation:
Pinto, V. A., Bortnik, J., Moya, P. S., Lyons, L. R., Sibeck, D. G., Kanekal, S. G., et al. (2018). Characteristics, occurrence, and decay rates of remnant belts associated with three-belt events in the Earth's radiation belts. *Geophysical Research Letters*, *45*. https://doi.org/10.1029/2018GL080274

Received 29 AUG 2018
Accepted 29 OCT 2018
Accepted article online 31 OCT 2018

Characteristics, Occurrence, and Decay Rates of Remnant Belts Associated With Three-Belt Events in the Earth's Radiation Belts

Victor A. Pinto[1], Jacob Bortnik[1], Pablo S. Moya[2], Larry R. Lyons[1], David G. Sibeck[3], Shrikanth G. Kanekal[3], Harlan E. Spence[4], and Daniel N. Baker[5]

[1]Department of Atmospheric and Oceanic Sciences, University of California, Los Angeles, CA, USA, [2]Departamento de Física, Facultad de Ciencias, Universidad de Chile, Santiago, Chile, [3]Heliophysics Science Division, NASA Goddard Space Flight Center, Greenbelt, MD, USA, [4]Institute for the Study of Earth, Oceans, and Space, University of New Hampshire, Durham, NH, USA, [5]Laboratory for Atmospheric and Space Physics, University of Colorado Boulder, Boulder, CO, USA

Abstract Shortly after the launch of the Van Allen Probes, a new three-belt configuration of the electron radiation belts was reported. Using data between September 2012 and November 2017, we have identified 30 three-belt events and found that about 18% of geomagnetic storms result in such configuration. Based on the identified events, we evaluated some characteristics of the remnant (intermediate) belt. We determined the energy range of occurrence and found it peaks at $E = 5.2$ MeV. We also determined that the magnetopause location and *SYM-H* value may play an important role in the outer belt losses that lead to formation and location of the remnant belt. Finally, we calculated the decay rates of the remnant belt for all events and found that their lifetime gets longer as energy increases, ranging from days at $E = 1.8$ MeV up to months at $E = 6.3$ MeV suggesting that remnant belts are extremely persistent.

Plain Language Summary One of the first results reported by the Van Allen Probes mission was the existence of a completely new configuration in which the electron outer radiation belt is split into two belts, resulting in a three-belt structure that has never been reported before. The uniqueness of this event has limited the studies that aim to explain the splitting of the belt, and therefore, the topic is controversial to this date. In this work we show that the occurrence of three-belt events is relatively common and therefore their formation and evolution process can be studied statistically. For the intermediate belt (remnant belt) we found two parameters that may influence their location and formation process. We have also calculated the time that the remnant belt would naturally last in absence of a strong external perturbation and found that the duration increases as the energy of the electrons increases.

1. Introduction

The Earth's electron radiation belts (Van Allen & Frank, 1959), located approximately between $1.2 < L < 7$, consist of a very stable inner zone, a *slot* region (Lyons & Thorne, 1973), and a very dynamic outer zone in which electron populations of energies from kilo electronvolt to mega electronvolt can vary by several orders of magnitude in periods ranging from hours to a few days (e.g., Baker et al., 2018; Reeves et al., 2016; Thorne, 2010). The outer zone extreme dynamics are ultimately driven by the solar wind interacting with the magnetosphere; therefore, the relation between geomagnetic storms (Gonzalez et al., 1994) and flux variations in the outer radiation belt has been extensively studied. It has been consistently found that while geomagnetic storms favor enhancements of electrons fluxes, they can also result in depletions or cause little variation to the outer belt electron populations (Kataoka & Miyoshi, 2006; Moya et al., 2017; Reeves et al., 2003; Turner et al., 2015; Yuan & Zong, 2012; Zhao & Li, 2013).

The Van Allen Probes mission was designed to study the radiation belts and to answer some of the many unknowns regarding their internal dynamics (Mauk et al., 2013). One of the first results of the mission was the discovery of a temporary third belt at high energies that lasted a month (Baker et al., 2013). The creation of this three-belt configuration was a product of a partial depletion of the outer belt that left a remnant belt at $2.8 < L < 3.5$and that was followed by a recovery of electron fluxes at $L > 4$ for energies > 3.4 MeV. To explain the formation of the remnant belt, Shprits et al. (2013, 2018) argued that simulation of losses by

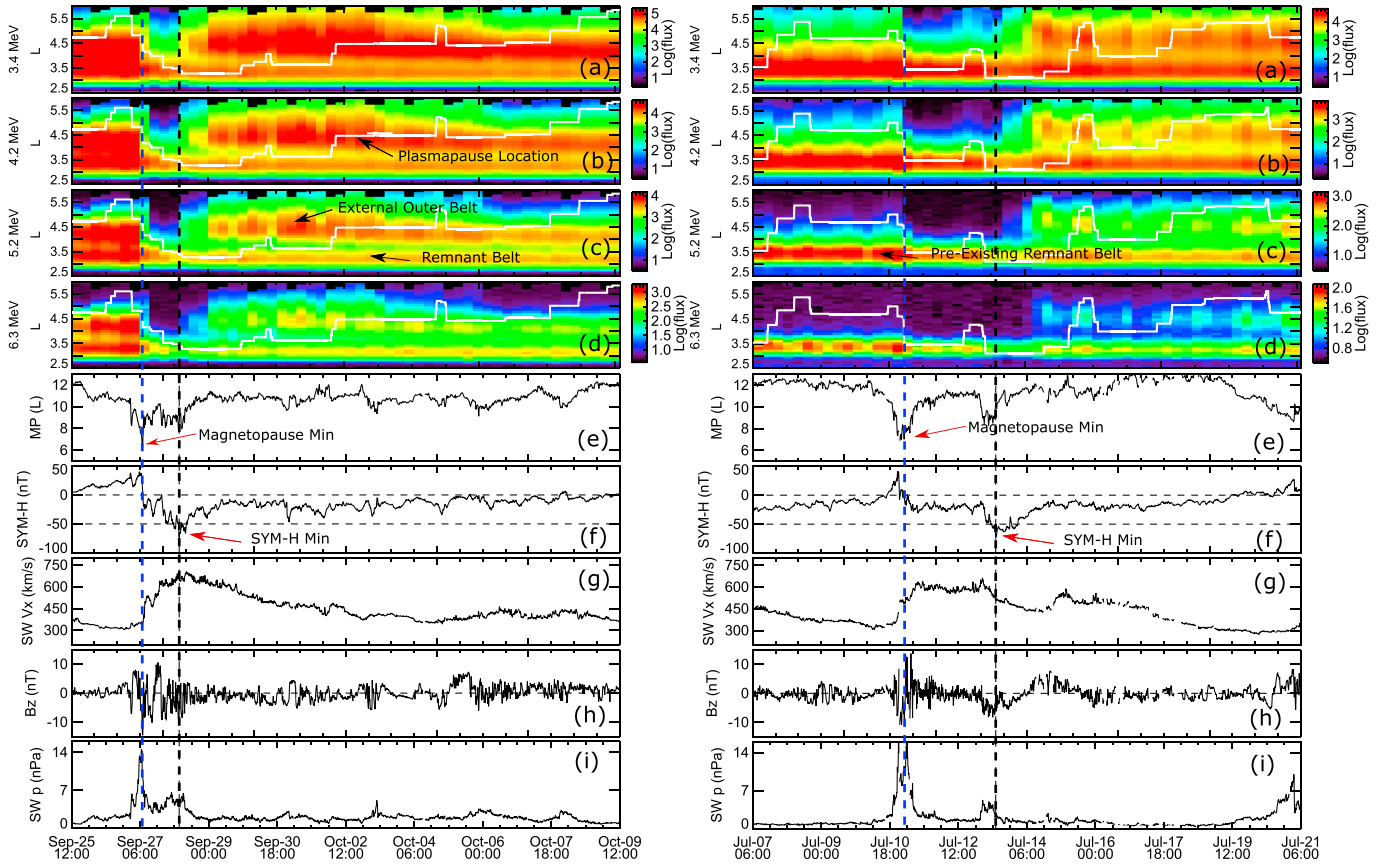

Figure 1. Example of a three-belt event that started 27 September 2017 (left column) and a second event that started on 13 July 2015 (right column). From top to bottom: spin-averaged combined electron fluxes from Van Allen Probes as a function of *L* for energy channels (a) 2.6, (b) 3.4, (c) 4.2, and (d) 5.2 MeV. Panel (e) corresponds to the estimated magnetopause standoff location and panel (f) to the *SYM-H* index. The bottom three panels show solar wind parameters such as speed V_x (g), IMF B_z (h), and dynamic pressure P_{dyn} (i). The blue dashed line corresponds to the time of magnetopause minimum. The black dashed line corresponds to *SYM-H* minimum.

scattering of electrons with electromagnetic ion-cyclotron (EMIC) waves can replicate the remnant belt formation, while Mann et al. (2016, 2018) has argued that electromagnetic ion-cyclotron wave scattering is not needed as losses to the magnetopause by a combination of inward motion of the magnetopause and fast outward diffusion driven by ultra low frequency waves was sufficient to replicate the observations. The decay of the remnant belt has been studied by Thorne et al. (2013) who argued that that a remnant belt trapped in the plasmasphere by a rapid expansion of the plasmapause will only present a slow decay, due to interactions with hiss waves.

To date, only few remnant belt events have been reported during the Van Allen Probes era (e.g., Baker et al., 2016; Kellerman et al., 2014), and no statistical analysis has been performed to characterize them. The most comprehensive studies come from Turner et al. (2013) who reported 13 double peak occurrences in phase space density of equatorially mirroring electrons between the years 2007 and 2011 using data from the Time History of Events and Macroscale Interactions during Substorms (THEMIS) spacecraft and from Yuan and Zong (2013) who reported eight three-belt events between the years 1994 and 2003 using data from the low-altitude Solar Anomalous and Magnetospheric Particle Explorer (SAMPEX) spacecraft. However, the different techniques, instruments, and measurements used both in Turner et al. (2013) and Yuan and Zong (2013) make it difficult to compare with Van Allen Probes era events. Additionally, the original September 2012 event reported is still the subject of disagreement with respect to the dominant process responsible for the formation of the remnant belt. In this work, for the first time we catalog three-belt events that occurred during the Van Allen Probes era, from September 2012 to November 2017. We report on the main characteristics of the events and discuss the process of decay of the remnant belt.

2. Data and Events

The Van Allen Probes have a highly elliptical (apogee ~5.8 R_E), near-equatorial (inclination ~10°) orbit with period ~9 hr. The satellites follow each other with separations that vary from ~1 hr to half-orbit; therefore, any particular radial distance gets is surveyed every few hours. To identify three-belt events, we have used spin-averaged electron flux data obtained from the Energetic Particle Composition and Thermal Plasma Suite (Spence et al., 2013) Relativistic Electron Proton Telescope (Baker et al., 2013) (ECT-REPT) on board the Van Allen Probes. We have combined the data from both satellites into a single grid of data points binned in space $\Delta L = 0.1$) and time ($\Delta t = 6$ hr) by averaging all data points available inside each bin, during the time period from 1 September 2012 to 30 November 2017. Here L corresponds to the dipole L (the radial distance at which a magnetic line would cross the equator). Solar wind data and magnetospheric indices have been obtained from the OMNI database. Magnetopause standoff location was calculated using the corrected Shue model (Shue et al., 1998).

Figure 1 (left column) shows a three-belt event that started on 27 September 2017 following a high-speed stream (HSS) arrival that resulted in a moderate geomagnetic storm (*SYM-H* minimum −74 nT). Panels (a) to (d) show the evolution of electron fluxes for energies between 2.6 and 5.2 MeV in the region $2.5 < L < 6$. Electron fluxes at $L > 3.5$ were depleted around the time a sharp increase in solar wind dynamic pressure arrived (panel i). As a result, a remnant belt stayed in place in $2.8 < L < 3.2$. The partial depletion was followed by an enhancement of the outer belt at higher L shells during the recovery phase of the storm that resulted in a stable three-belt configuration (inner belt is not shown). Panel (e) shows that with the arrival of the high-speed stream the magnetopause standoff location briefly moved down to $L = 6.0$ (27 September 2017 07:30 UT), which match with the time of the partial depletion. The three-belt configuration lasted until 11 October 2017 when another high-speed stream-driven storm completely depleted the outer belt (not shown). Plasmapause location calculated by the AE-dependent (O'Brien & Moldwin, 2003) empirical model (shown in panels (a) to (d) as a white line) defines with relative accuracy the penetration and the initial depletion after the arrival of the high-speed stream, suggesting that a plasmapause effect may prevent a complete disappearance of the outer belt and therefore help the *formation* of a remnant belt. The plasmapause location moves outward in the following days, consistent with the idea that the remnant belt can remain in place if it is shielded from loss and acceleration processes outside the plasmapause that result in the creation of the new external outer belt. Figure 1 (right column) shows another three-belt event that started around 13 July 2015 also in association with a moderate storm resulting of the arrival of a high-speed stream on 10 July 2015 and a small coronal mass ejection (CME) on 13 July 2015 (*SYM-H* minimum −71). In this case the magnetopause was also pushed inward down to $L = 6.3$ in association with a sharp increase in solar wind dynamic pressure. In this event, a preexisting remnant belt was already in place and was affected only moderately by the pressure shock arrival, and only after a few days the formation of the new outer belt lead to a three-belt event.

For the period between September 2012 and November 2017, we found 30 events that present a three-belt structure, defined as an extended period of time (>1 day or about three satellite orbits) in which a double peak in flux versus L is observed beyond the slot region at $L = 3$, in at least one energy channel in the range $1.8 \leq E \leq 7.6$ MeV. We checked all energy channels individually to determine if there is a triple belt or a remnant belt only. We have listed all the dates, *SYM-H* minimum for each event, the interplanetary driver associated with each event, magnetopause minimum location, the range of energies at which each event presents a three-belt structure, and whether there was a preexisting remnant belt or not in the suporting information.

3. General Characteristics of Three-Belt Events

Three-belt events occur under a variety of geomagnetic conditions, associated with high-speed streams (HSS) that either result in geomagnetic storms (13 events or 43%) or do not (10 events or 33%), while other events are associated with CME-driven storms (five events or 17%) and finally some occur in association with geomagnetic storms that resulted from the combination of CME and HSS (two events or 7%). If we consider all geomagnetic storms that occurred between September 2012 and November 2017, the fraction that resulted in three-belt events was 13 of 46 (28%) for high-speed streams , 5 of 48 (10%) for CMEs, and 2/15 (13%) for CME + HSS storms. These numbers, when combined, indicate that 18% of all geomagnetic storms lead to three-belt events. We have not calculated the occurrence rate for high-speed streams not resulting in geomagnetic storms, but these do occur, a result that is consistent with the current notion that a traditional geomagnetic storm is not needed to drive an enhancement of electrons in the radiation belts (e.g., Kim et al., 2015; Pinto et al., 2018; Schiller et al., 2014).

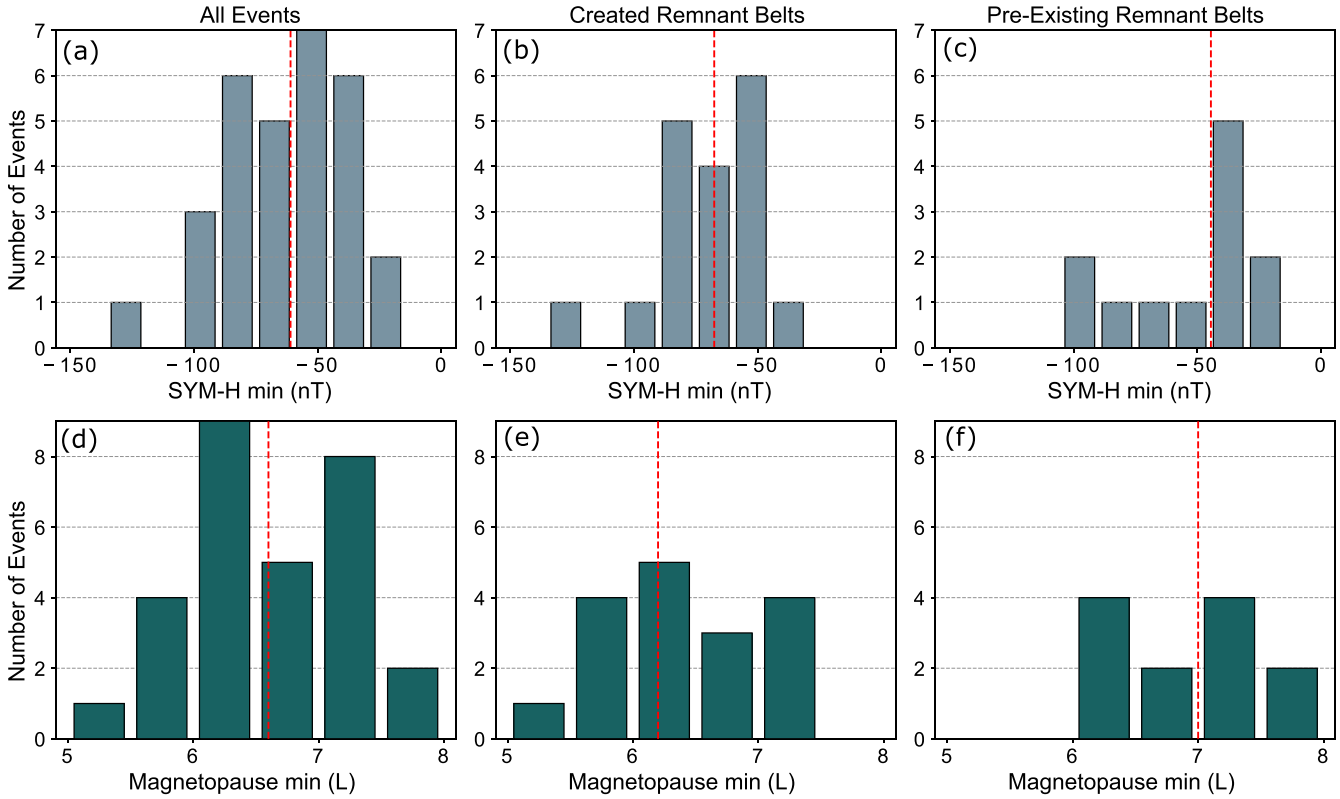

Figure 2. *SYM-H* minimum (top) and magnetopause standoff minimum *L* value (bottom) calculated during 48 hr before and after of each event at time $t = 0$ for all events (a, d), events in which the remnant belt is created (b, e), and events with a preexisting remnant belt (c, f). Red dashed lines correspond to the median value of the distributions.

For the outer radiation belts to enter a three-belt configuration, a combination of two different and in principle independent processes must occur. First, a remnant belt should be created, either abruptly as the result of a fast depletion of the fluxes at high *L* shells or through a slower process of erosion of the existing outer belt that can occur in days to months. Second, a new *external outer* belt must form at higher *L* shells following the depletion but occurring in a region that does not overlap or significantly affect the dynamics of the already established remnant belt, so that the two populations can coexist. Oftentimes, both processes occur as a consequence of a single geomagnetic disturbance, but it is also possible to have large time delays between the creation of the remnant belt and the appearance of the new outer belt. We are interested in the consequences of the process of formation of the remnant belt, as it has been proposed that the magnetopause location may play a role in the formation of remnant belts (Mann et al., 2016, 2018). To do this, we have separated the events by the change in the location of the peak of the radiation belt fluxes. Events with a partial depletion leave behind a remnant belt that experiences a quick inward motion of the peak in flux, while events with a preexisting remnant belt see no change (or minimal change) in the location of the peak in flux after the commencement of the relevant geomagnetic disturbance has occurred. We have chosen a threshold of $\Delta = 0.3L$ to determine if an event corresponds to the group of *preexisting* remnant belt or *created* remnant belt as that particular number describes with relative accuracy that we visually observe in the data. Figure 2 presents a histogram of the magnetopause standoff minimum *L* values calculated within 48 hr of the start of each event and *SYM-H* minimum in the same time window. The left column corresponds to the distribution of values for all events, while the middle and right columns correspond to the separation between events in which the remnant belt was created versus events in which the remnant belt can be considered preexisting.

The *SYM-H* minimum distribution in Figure 2a shows that three-belt events occur in a variety of weak to moderate geomagnetic storms, with a median value of the distribution of −61 nT. Here only one event occurs for *SYM-H* minimum significantly lower than −100 nT. If we separate the events, we find that cases in which the remnant belt is created (b) present a higher *SYM-H* drop with a median value of −68 nT, while preexisting remnant belt cases tend to develop under weak (or no) storms, with a median value of −45 nT (c). This may

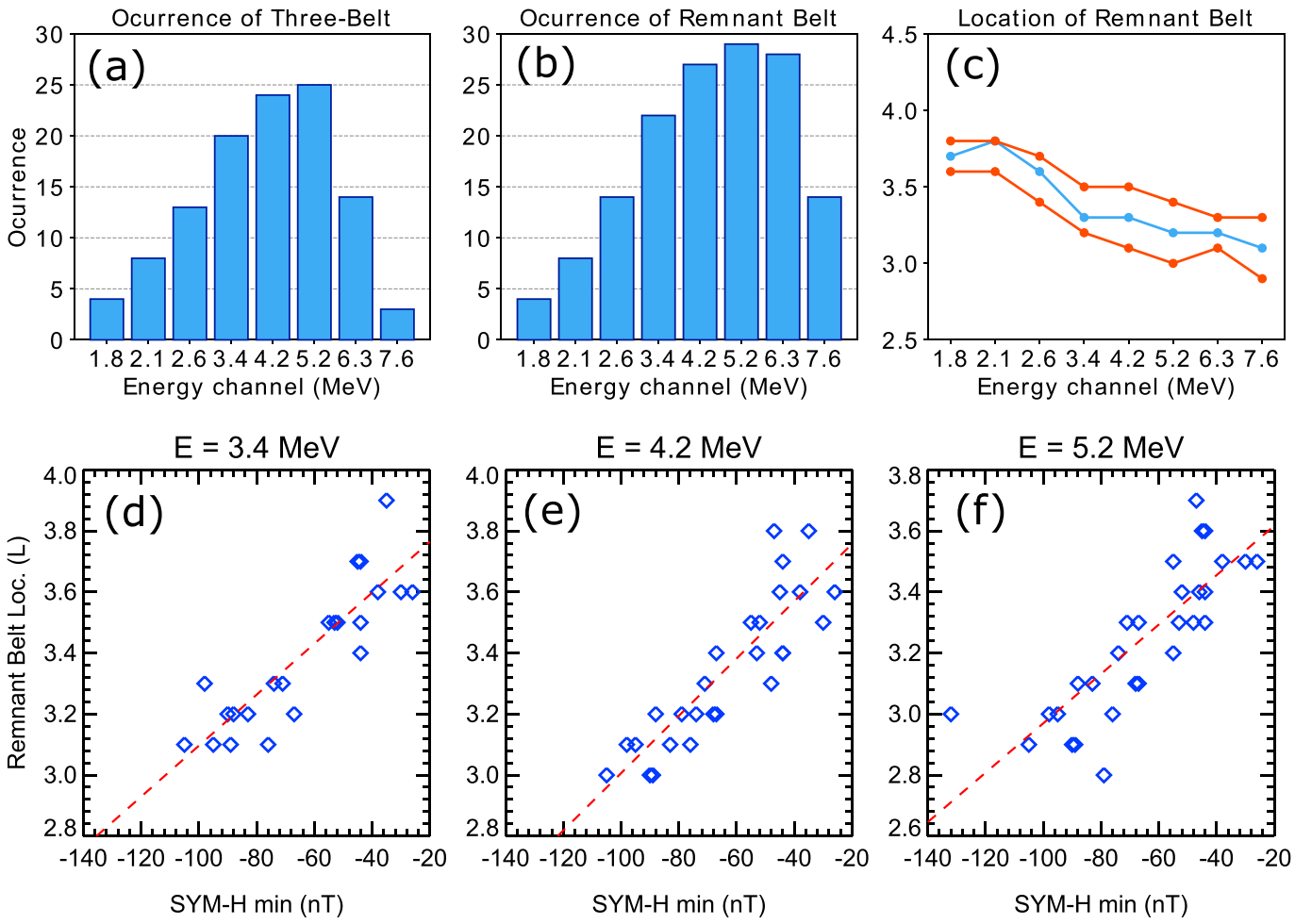

Figure 3. Top row: observed occurrence frequency of three-belt events (a) and remnant belts (b) and peak location of remnant belts as a function of energy (c) with blue line corresponding to median value and red corresponding to quartiles. Bottom row: relationship between *SYM-H* minimum and remnant belt peak location (*L*) for energy channels 3.4 (d), 4.2 (e), and 5.2 MeV (f). Red dashed line corresponds to the best linear fit for the trend.

reflect weak storms not being able to produce depletion of fluxes down to very low *L* shells but still resulting in enhancements at higher *L* shells. The estimated minimum location of the magnetopause results in a broad distribution (d) covering $5.0 < L < 8.1$ (median $L = 6.6$), the subset of events during which the remnant belt is created (e) can be generally associated with lower magnetopause standoff locations (median $L = 6.2$) than events with a preexisting (f) remnant belt ($L = 7.0$), which is consistent with the idea of a magnetopause influence on the formation of the remnant belts.

Remnant belts tend to be observed in more energy channels than three belt s. One possible explanation is that since remnant belt creation and enhancement of the outer belt are different processes, it may be easier for a disturbance to remove those particles at high energies than it is to repopulate them in the outer region. Figure 3a shows the observed occurrence of three-belt events as a function of the energy of the electrons. The occurrence rate increases with energy, peaks at $E = 5.2$ MeV and then greatly decreases at higher energies. Figure 3b shows the occurrence of remnant belts. Similar to the events with a three-belt structure, remnant belt occurrence also peaks at $E = 5.2$ MeV; however, remnant belt occurrence tends to remain higher at high energies when comparing to three-belt events. Figure 3c shows the median location of the peak of the remnant belt (blue) for all events, as well as the upper and lower quartiles (red). The location of the remnant belt shows dependence on the energy of the particles, the median location decreasing in *L* shell as the energy increases from $L = 3.9$ for $E = 1.8$ MeV to $L = 2.9$ at $E = 7.6$ MeV.

We have also explored the dependence of the remnant belt location with respect to geomagnetic indices and found that *SYM-H* shows the best correlation with the location of remnant belts. Figures 3d–3f show the

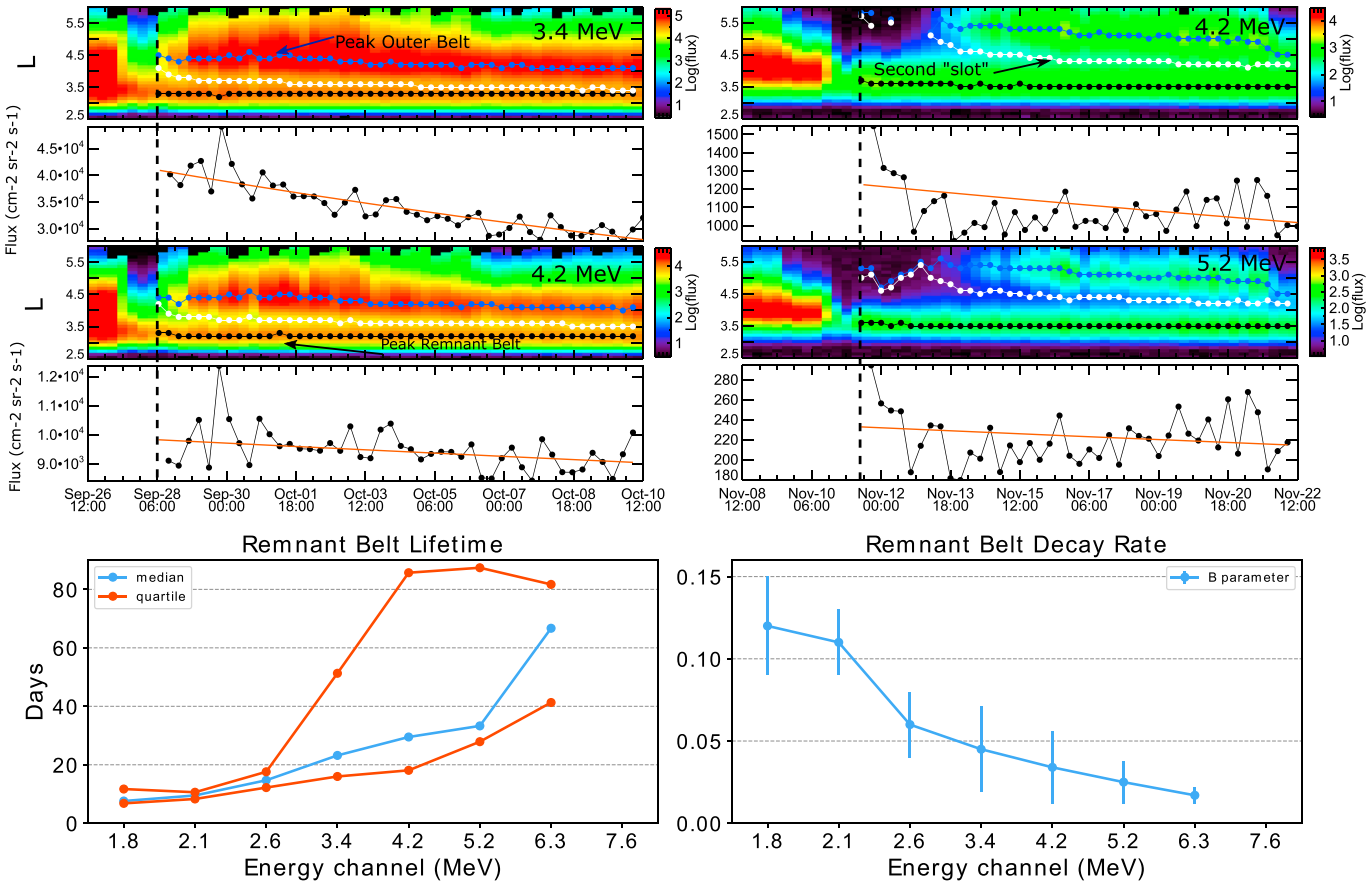

Figure 4. Location of the remnant belt (black dots), external slot (white dots), and outer belt peak flux (blue dots) for two events that occurred on 26 September 2017 (left column) and 10 November 2016 (right column) for two different energy channels. Below each plot there is a time series that show the flux values for the remnant belt peak and the best fit of the decay rate. Bottom panels correspond to the lifetime of the remnant belt as a function of energy for all events (left) and *B* parameter (right).

SYM-H minimum versus the location of the remnant belt for all events for three different energy channels. The linear trend has been marked as a red dashed line, and the correlation coefficient of the linear trend has been calculated as 0.87 for $E = 3.4$ MeV (d), 0.87 for $E = 4.2$ MeV (e), and 0.81 for $E = 5.2$ MeV (f). The location of the peak flux in the outer radiation belt after a storm is known to correlate with the *SYM-H* index (Moya et al., 2017; Tverskaya et al., 2003), but the correlation for the remnant belt is probably associated with the partial depletion of the belt at the beginning of the events.

4. On the Persistence and Decay of the Remnant Belt

Remnant belts can be very persistent. A strong geomagnetic storm could certainly destroy the remnant belt, but otherwise, they naturally decay slowly as they appear to be relatively shielded from loss processes during moderate geomagnetic activity, in particular, at high energies; therefore, the duration of a three-belt event depends principally on the ability of the external outer radiation belt to survive, which tends to decay relatively quickly. The duration of three-belt events in our list ranges from 5 to 17 days with an average duration of 11 days at $E = 4.2$ MeV, while the duration of the remnant belts can be occasionally measured in months (An example of a long-lasting remnant belt can be found in the supporting information). To estimate the lifetime of the remnant belts, we have calculated the decay rate assuming that the electrons follow an exponential decay given by

$$f(t) = Ae^{-Bt},$$

where f corresponds to the electron flux measured in $cm^{-2}sr^{-1}s^{-1}$ and A and B are the parameters to fit. To find the best fit, we first identified the peak flux location of every remnant belt for every energy channel and then performed a linear fit to the natural logarithm of the peak fluxes of the remnant belt. We have chosen the start time of the event at the vertical dashed line in Figures 1 and 4, which corresponds to the minimum

SYM-H value of the associated geomagnetic disturbance. Because we are interested in the natural decay rate of the remnant belt, we have excluded from the calculation the depletion associated with the start of the event; therefore, the fitting must start after $t = 0$ (vertical dashed line). Figure 4 shows an example of the peak location of the remnant belt and the decay rate for two energy channels for the event shown in Figure 1 and for a second event that occurred on 10 November 2016. The upper panels show fluxes for two energies as a function of *L*, and we have overplotted the remnant belt peak (black), the minimum of the external slot (white) region, and the new external outer belt peak flux (blue). The peak electron fluxes of the remnant belt for the shown energy channels are shown below each plot along with the linear fit of the data (shown in red).

To calculate the lifetime of the remnant belt, we have excluded fluxes that are too low $f < 25\ \mathrm{cm}^{-2} \cdot \mathrm{sr}^{-1} \cdot \mathrm{s}^{-1}$ as they approach the background noise level of the REPT instrument (Claudepierre et al., 2015). We have also ignored those events that do not present a decay but rather a growth in flux. Events with growth rates in flux instead of decay tend to present very small growth and can be due to fluctuations on the data associated with the location of the spacecraft or acceleration processes that in fact supply particles to the remnant belt region, but these cases are beyond the scope of the present study. The values of the remnant belt lifetime and the parameter *B* for every energy channel can be found in the supporting information. Individual fit parameters for every events are available in the supporting information. Figure 4 (bottom left) shows the lifetime (in days) of the remnant belt calculated for different energy channels and the value of the fit parameter *B* (bottom right). It can be seen that the lifetime of the remnant belt increases as a function of the energy, yet while the lower quartile and median values tend to present only moderate variation, there are a number of events in which the lifetime is very high especially at energies of 4.2 MeV and higher, indicating that, in general, remnant belts are indeed very stable. We consider those values to be in agreement with previous studies that have evaluated the decay rates of the outer radiation belt (e.g., Drozdov et al., 2015; Thorne et al., 2013).

5. Summary, Discussion, and Conclusions

The discovery of the third radiation belt (Baker et al., 2013) has generated much interesting discussion about the possible causes leading to such a configuration; however, to date, there have been a limited number of events reported and no extensive statistical examination of such events. Here we have identified 30 three-belt events, between September 2012 and November 2017. We have shown that around 18% of all geomagnetic storms during that period of time led to a remnant belt or three-belt structure, usually at energies between 3.4 and 5.2 MeV making this a relatively common phenomena that can be statistically studied. The variety of geomagnetic conditions under which three-belt events can occur suggests that there may be more than one process responsible for the formation and evolution of three-belt events. In particular, the magnetopause location might have a stronger role in events that are created, while preexisting events may be the result of more natural long-term decay process occurring in the outer radiation belt. Although the same can be said about *SYM-H* minimum which more strongly correlates with the location of the remnant belts, the *SYM-H* effect seems to be general to all events and therefore should be explored further. Although three-belt events occur more often during weak to moderate storms, they can also occur in association with high-speed streams that cause no storm.

As there is still relatively little known about three-belt events, we have tried to characterize them based on a number of parameters: the energy at which they appear, the conditions that lead to their formation, and the boundaries that are thought to be important in their dynamics, such as the magnetopause location, in part motivated by early studies that present those parameter as being of possible importance. By calculating the decay rate of the remnant belt after it is formed, we can conclude that while a three-belt event can vary between a few days to a few weeks depending on the particularities of each event and the energy of the electrons, remnant belts can exist in the radiation belts for months and possibly years given that no other strong storm removes them from existence. This is in agreement with Thorne et al.'s (2013) suggestion that pitch angle scattering with hiss waves is the responsible for decay of remnant belts. Of course, this assumes that the remnant belt is located inside the plasmasphere and therefore shielded from other interactions, but an extensive study of the effects of the plasmapause in three-belt events is yet to be performed. Three-belt events and remnant belts preferentially occur at energies between 3.4 and 5.2 MeV, but there are a significant number of events outside that energy range, and therefore, it seems to be an important topic for discussion if the mechanisms that favor formation of remnant belts at 1.8 MeV are the same that are dominating at 7.6 MeV.

Three-belt structures represent a unique configuration of the radiation belts which comes about as a consequence of a number of factors that deplete and enhance fluxes of energetic electrons in the radiation belts.

The processes are in general energy dependent and location specific, and as such, an important challenge is to understand and untangle the effects of the contributing mechanisms. This letter is the first attempt to understand the characteristics of the events. For example, instead of using phase space density (to separate adiabatic from non adiabatic effects), we have chosen to use fluxes so our results can be more directly comparable to previous studies that also dealt with fluxes (e.g., Baker et al., 2013), and because our objective was to characterize and study the statistical behavior of the remnant belts. Phase space density studies will be required in order to unravel the relevant physical processes responsible for acceleration and losses leading to this particular configuration. Our results provide valuable insights about the characteristics of three-belt events and their relationship with geomagnetic boundaries and indices and contribute to the understanding of the response of the radiation belts to the effects of the solar wind.

Acknowledgments
We acknowledge NASA/GSFC's Space Physics Data Facility's OMNIWeb and CDAWeb services and OMNI data for providing Solar Wind data (https://cdaweb.sci.gsfc.nasa.gov/) and the Van Allen Probes ECT-REPT team. REPT data were obtained from SODC (https://www.rbsp-ect.lanl.gov/). V. A. P. thanks the support of Becas Chile program. J. B. would like to acknowledge NASA awards NNX16AG21G and NNX14AN85G and AFOSR award FA9550-15-1-0158. P. S. M. is grateful for the support of CONICyT Chile FONDECyT grant 11150055 and Conicyt PIA project ACT1405.

References

Baker, D. N., Erickson, P. J., Fennell, J. F., Foster, J. C., Jaynes, A. N., & Verronen, P. T. (2018). Space weather effects in the Earth's radiation belts. *Space Science Reviews*, *214*(1). https://doi.org/10.1007/s11214-017-0452-7

Baker, D. N., Jaynes, A. N., Kanekal, S. G., Foster, J. C., Erickson, P. J., Fennell, J. F., et al. (2016). Highly relativistic radiation belt electron acceleration, transport, and loss: Large solar storm events of March and June 2015. *Journal of Geophysical Research: Space Physics*, *121*, 6647–6660. https://doi.org/10.1002/2016JA022502

Baker, D. N., Kanekal, S. G., Hoxie, V. C., Batiste, S., Bolton, M., Li, X., et al. (2013). The relativistic electron-proton telescope (REPT) instrument on board the radiation belt storm probes (RBSP) spacecraft: Characterization of Earth's radiation belt high-energy particle populations. *Space Science Reviews*, *179*(1-4), 337–381. https://doi.org/10.1007/s11214-012-9950-9

Baker, D. N., Kanekal, S. G., Hoxie, V. C., Henderson, M. G., Li, X., Spence, H. E., et al. (2013). A long-lived relativistic electron storage ring embedded in Earth's outer Van Allen belt. *Science*, *340*(6129), 186–190. https://doi.org/10.1126/science.1233518

Claudepierre, S. G., O'Brien, T. P., Blake, J. B., Fennell, J. F., Roeder, J. L., Clemmons, J. H., et al. (2015). A background correction algorithm for Van Allen Probes MagEIS electron flux measurements. *Journal of Geophysical Research: Space Physics*, *120*, 5703–5727. https://doi.org/10.1002/2015JA021171

Drozdov, A. Y., Shprits, Y. Y., Orlova, K. G., Kellerman, A. C., Subbotin, D. A., Baker, D. N., et al. (2015). Energetic, relativistic, and ultrarelativistic electrons: Comparison of long-term VERB code simulations with Van Allen Probes measurements. *Journal of Geophysical Research: Space Physics*, *120*, 3574–3587. https://doi.org/10.1002/2014JA020637

Gonzalez, W. D., Joselyn, J. A., Kamide, Y., Kroehl, H. W., Rostoker, G., Tsurutani, B. T., & Vasyliunas, V. M. (1994). What is a geomagnetic storm? *Journal of Geophysical Research*, *99*(A4), 5771–5792. https://doi.org/10.1029/93JA02867

Kataoka, R., & Miyoshi, Y. (2006). Flux enhancement of radiation belt electrons during geomagnetic storms driven by coronal mass ejections and corotating interaction regions. *Space Weather*, *4*, S09004. https://doi.org/10.1029/2005SW000211

Kellerman, A. C., Shprits, Y. Y., Kondrashov, D., Subbotin, D., Makarevich, R. A., Donovan, E., & Nagai, T. (2014). Three-dimensional data assimilation and reanalysis of radiation belt electrons: Observations of a four-zone structure using five spacecraft and the VERB code. *Journal of Geophysical Research: Space Physics*, *119*, 8764–8783. https://doi.org/10.1002/2014JA020171

Kim, H.-J., Lyons, L., Pinto, V., Wang, C.-P., & Kim, K.-C. (2015). Revisit of relationship between geosynchronous relativistic electron enhancements and magnetic storms. *Geophysical Research Letters*, *42*, 6155–6161. https://doi.org/10.1002/2015GL065192

Lyons, L. R., & Thorne, R. M. (1973). Equilibrium structure of radiation belt electrons. *Journal of Geophysical Research*, *78*(13), 2142–2149. https://doi.org/10.1029/JA078i013p02142

Mann, I. R., Ozeke, L. G., Morley, S. K., Murphy, K. R., Claudepierre, S. G., Turner, D. L., et al. (2018). Reply to 'The dynamics of Van Allen belts revisited'. *Nature Physics*, *14*(2), 103–104. https://doi.org/10.1038/nphys4351

Mann, I. R., Ozeke, L. G., Murphy, K. R., Claudepierre, S. G., Turner, D. L., Baker, D. N., et al. (2016). Explaining the dynamics of the ultra-relativistic third Van Allen radiation belt. *Nature Physics*, *12*(10), 978–983. https://doi.org/10.1038/nphys3799

Mauk, B. H., Fox, N. J., Kanekal, S. G., Kessel, R. L., Sibeck, D. G., & Ukhorskiy, A. (2013). Science objectives and rationale for the radiation belt storm probes mission. *Space Science Reviews*, *179*(1-4), 3–27. https://doi.org/10.1007/s11214-012-9908-y

Moya, P. S., Pinto, V. A., Sibeck, D. G., Kanekal, S. G., & Baker, D. N. (2017). On the effect of geomagnetic storms on relativistic electrons in the outer radiation belt: Van allen probes observations. *Journal of Geophysical Research: Space Physics*, *122*, 11,100–11,108. https://doi.org/10.1002/2017JA024735

O'Brien, T. P., & Moldwin, M. B. (2003). Empirical plasmapause models from magnetic indices. *Geophysical Research Letters*, *30*(4), 1152. https://doi.org/10.1029/2002GL016007

Pinto, V. A., Kim, H.-J., Lyons, L. R., & Bortnik, J. (2018). Interplanetary parameters leading to relativistic electron enhancement and persistent depletion events at geosynchronous orbit and potential for prediction. *Journal of Geophysical Research: Space Physics*, *123*, 1134–1145. https://doi.org/10.1002/2017JA024902

Reeves, G. D., Friedel, R. H. W., Larsen, B. A., Skoug, R. M., Funsten, H. O., Claudepierre, S. G., et al. (2016). Energy-dependent dynamics of keV to MeV electrons in the inner zone, outer zone, and slot regions. *Journal of Geophysical Research: Space Physics*, *121*, 397–412. https://doi.org/10.1002/2015JA021569

Reeves, G. D., McAdams, K. L., Friedel, R. H. W., & O'Brien, T. P. (2003). Acceleration and loss of relativistic electrons during geomagnetic storms. *Geophysical Research Letters*, *30*(10), 1529. https://doi.org/10.1029/2002GL016513

Schiller, Q., Li, X., Blum, L., Tu, W., Turner, D. L., & Blake, J. B. (2014). A nonstorm time enhancement of relativistic electrons in the outer radiation belt. *Geophysical Research Letters*, *41*, 7–12. https://doi.org/10.1002/2013GL058485

Shprits, Y. Y., Horne, R. B., Kellerman, A. C., & Drozdov, A. Y. (2018). The dynamics of Van Allen belts revisited. *Nature Physics*, *14*(2), 102–103. https://doi.org/10.1038/nphys4350

Shprits, Y. Y., Subbotin, D., Drozdov, A., Usanova, M. E., Kellerman, A., Orlova, K., et al. (2013). Unusual stable trapping of the ultrarelativistic electrons in the Van Allen radiation belts. *Nature Physics*, *9*(11), 699–703. https://doi.org/10.1038/nphys2760

Shue, J.-H., Song, P., Russell, C. T., Steinberg, J. T., Chao, J. K., Zastenker, G., et al. (1998). Magnetopause location under extreme solar wind conditions. *Journal of Geophysical Research*, *103*(A8), 17,691–17,700. https://doi.org/10.1029/98JA01103

Spence, H. E., Reeves, G. D., Baker, D. N., Blake, J. B., Bolton, M., Bourdarie, S., et al. (2013). Science goals and overview of the radiation belt storm probes (RBSP) energetic particle, composition, and thermal plasma (ECT) suite on NASA's Van Allen probes mission. *Space Science Reviews*, *179*(1-4), 311–336. https://doi.org/10.1007/s11214-013-0007-5

Thorne, R. M. (2010). Radiation belt dynamics: The importance of wave-particle interactions. *Geophysical Research Letters*, *37*, L22107. https://doi.org/10.1029/2010GL044990

Thorne, R. M., Li, W., Ni, B., Ma, Q., Bortnik, J., Baker, D. N., et al. (2013). Evolution and slow decay of an unusual narrow ring of relativistic electrons near L 3.2 following the September 2012 magnetic storm. *Geophysical Research Letters*, *40*, 3507–3511. https://doi.org/10.1002/grl.50627

Turner, D. L., Angelopoulos, V., Li, W., Hartinger, M. D., Usanova, M., Mann, I. R., et al. (2013). On the storm-time evolution of relativistic electron phase space density in Earth's outer radiation belt. *Journal of Geophysical Research: Space Physics*, *118*, 2196–2212. https://doi.org/10.1002/jgra.50151

Turner, D. L., O'Brien, T. P., Fennell, J. F., Claudepierre, S. G., Blake, J. B., Kilpua, E. K. J., & Hietala, H. (2015). The effects of geomagnetic storms on electrons in Earth's radiation belts. *Geophysical Research Letters*, *42*, 9176–9184. https://doi.org/10.1002/2015GL064747

Tverskaya, L. V., Pavlov, N. N., Blake, J. B., Selesnick, R. S., & Fennell, J. F. (2003). Predicting the L-position of the storm-injected relativistic electron belt. *Advances in Space Research*, *31*(4), 1039–1044. https://doi.org/10.1016/S0273-1177(02)00785-8

Van Allen, J. A., & Frank, L. A. (1959). Radiation around the Earth to a radial distance of 107,400 km. *Nature*, *183*(4659), 430–434. https://doi.org/10.1038/183430a0

Yuan, C. J., & Zong, Q.-G. (2012). Quantitative aspects of variations of 1.5-6.0 MeV electrons in the outer radiation belt during magnetic storms. *Journal of Geophysical Research*, *117*, A11208. https://doi.org/10.1029/2011JA017346

Yuan, C., & Zong, Q. (2013). The double-belt outer radiation belt during CME- and CIR-driven geomagnetic storms. *Journal of Geophysical Research: Space Physics*, *118*, 6291–6301. https://doi.org/10.1002/jgra.50564

Zhao, H., & Li, X. (2013). Inward shift of outer radiation belt electrons as a function of Dst index and the influence of the solar wind on electron injections into the slot region. *Journal of Geophysical Research: Space Physics*, *118*, 756–764. https://doi.org/10.1029/2012JA018179